European Journal of Nuclear Medicine and Molecular Imaging (2025) 52:2431–2443
https://doi.org/10.1007/s00259-025-07102-8

ORIGINAL ARTICLE

Biodistribution and dosimetry of [^{177}Lu]Lu-SibuDAB in patients with metastatic castration-resistant prostate cancer

Philipp Ritt[1,2] · René Fernández[3] · Cristian Soza-Ried[3,4] · Heinz Nicolai[3,5] · Horacio Amaral[3,6] · Korbinian Krieger[7,8] · Ana Katrina Mapanao[7] · Amanda Rotger[1] · Konstantin Zhernosekov[1] · Roger Schibli[7,8] · Cristina Müller[7,8] · Vasko Kramer[3,6]

Received: 23 September 2024 / Accepted: 17 January 2025 / Published online: 3 February 2025

Abstract

Purpose Several prostate-specific membrane antigen (PSMA) radiopharmaceuticals have been used for the treatment of metastatic, castration-resistant prostate cancer (mCRPC). In an attempt to improve the tumour accumulation, new PSMA ligands were developed with an albumin-binding entity to enhance the blood circulation and, hence, tumour accumulation. In preclinical studies, [^{177}Lu]Lu-SibuDAB, a radiopharmaceutical with moderate albumin-binding properties, outperformed [^{177}Lu]Lu-PSMA-617 and [^{177}Lu]Lu-PSMA-I&T. The aim of this study was to evaluate the dosimetry of [^{177}Lu]Lu-SibuDAB in patients diagnosed mCRPC.

Methods Seventeen patients (median age 72 years, range 63−83) diagnosed with progressive disease of mCRPC were included in this prospective study after exhausting all available treatment options. They were injected with 5.3 ± 0.5 GBq (mean ± standard deviation) [^{177}Lu]Lu-SibuDAB as a first treatment cycle. Sixteen of these patients underwent sequential whole-body SPECT/CT and activity determination in venous blood samples for dosimetry purposes. Absorbed doses to the salivary glands, liver, spleen, kidneys, and red marrow as well as selected tumour lesions were calculated in OLINDA/EXM™ and compared to published values for previously established PSMA radiopharmaceuticals.

Results Absorbed dose coefficients (ADC) to tumours (9.9 ± 5.4 Gy/GBq) were about 2-fold higher than those reported for clinically approved PSMA radiopharmaceuticals. ADC to salivary glands, liver, spleen, kidneys and red marrow were higher (0.5 ± 0.2, 0.2 ± 0.05, 0.2 ± 0.1, 1.8 ± 0.6, 0.1 ± 0.04 Gy/GBq, respectively) than for [^{177}Lu]Lu-PSMA-617 and [^{177}Lu]Lu-PSMA-I&T, but lower than for [^{177}Lu]Lu-PSMA-ALB-56, a previously investigated long-circulating PSMA radiopharmaceutical. The tumour-to-kidneys, tumour-to-red marrow, tumour-to-salivary glands ADC ratio were 6.6, 102, 33.1. These ratios were comparable to those of [^{177}Lu]Lu-PSMA-617 and [^{177}Lu]Lu-PSMA-I&T for kidneys and red-marrow, but higher for salivary glands.

Conclusion [^{177}Lu]Lu-SibuDAB showed a prolonged blood circulation time and, hence, a significantly increased absorbed tumour dose, while tumour-to-organ ADC ratios were similar to conventional PSMA radiopharmaceuticals. Further clinical investigations to evaluate the efficacy and safety of [^{177}Lu]Lu-SibuDAB are, thus, warranted.

Keywords [^{177}Lu]Lu-SibuDAB · Radiopharmaceutical therapy · Albumin binder · MCRPC · Prostate cancer · Dosimetry

Introduction

Prostate cancer is the most frequently diagnosed type of cancer in men and the second most common neoplastic cause of premature death [1]. The prostate-specific membrane antigen (PSMA) is expressed in the healthy prostate secretory acinar epithelium and overexpressed in the plasma membrane of prostate cancer cells. It has been reported that PSMA expression correlates positively with high-grade, metastatic, and castration-resistant disease [2–4]. Therefore, PSMA has been proven to be a valid target for radiopharmaceutical therapy (RPT) of metastatic, castration-resistant prostate cancer (mCRPC) [5, 6]. The positive outcome of ^{177}Lu-based RPT applied over the last decade [7–11] and a Phase III clinical trial (VISION; NCT03511664) [12] resulted in the approval of [^{177}Lu]Lu-PSMA-617 (Pluvicto™, Novartis) by the Food and Drug Administration and the European Medicines Agency [12].

Extended author information available on the last page of the article

Recent preclinical efforts have been focused on the development of novel PSMA radiopharmaceuticals functionalised with a *p*-iodophenyl-entity which binds with high affinity to serum albumin [13]. The rationale of this concept was to prolong the blood circulation time and, thus, increase the tumour uptake of the otherwise rapidly excreted radiopharmaceuticals [14–16]. Indeed, the tumour accumulation was significantly improved, however, these promising findings were overshadowed by overly high blood activity levels and increased renal retention of activity. [^{177}Lu]Lu-PSMA-ALB-56 was the first PSMA radiopharmaceutical modified with a *p*-tolyl-entity [15], which binds with over 10-fold lower affinity to serum albumin than the *p*-iodophenyl-entity [13]. The favourable distribution profile of [^{177}Lu]Lu-PSMA-ALB-56 in preclinical mouse models translated in considerably enhanced therapeutic efficacy as compared to that of [^{177}Lu]Lu-PSMA-617 [15]. In a prospective study conducted at the Center for Nuclear Medicine, Positronmed in Santiago de Chile, Chile, [^{177}Lu]Lu-PSMA-ALB-56 was administered with an average activity of 3.4 ± 0.4 GBq per treatment cycle to patients with progressive mCRPC and no other treatment options [17]. It was well tolerated, and no severe adverse events were observed. Although the tumour absorbed dose was considerably enhanced, the activity level in the blood was about one order of magnitude higher than for [^{177}Lu]Lu-PSMA-617 and [^{177}Lu]Lu-PSMA-I&T, resulting in considerably increased bone marrow absorbed dose. The kidney absorbed dose was also unfavourably increased, however, the salivary glands dose was similar to that of established radiopharmaceuticals resulting in tumour-to-salivary gland absorbed dose coefficient (ADC) ratios that were almost doubled as compared to those of conventional radiopharmaceuticals [17].

Aiming at further optimization of the radioligand design, a new generation of PSMA radiopharmaceuticals was established with (*S*)-ibuprofen as an albumin-binding entity [18]. Preclinical studies have shown that the enantiopure [^{177}Lu]Lu-(*S*)-Ibu-DAB-PSMA is a promising candidate in terms of tumour-to-normal-organ ADC ratios, which outperformed those of the enantiopure [^{177}Lu]Lu-(*R*)-Ibu-DAB-PSMA with R-ibuprofen, the racemic [^{177}Lu]Lu-Ibu-DAB-PSMA, and [^{177}Lu]Lu-PSMA-ALB-56. In a therapy study with mice bearing PSMA-positive PC-3 PIP tumour xenografts, [^{177}Lu]Lu-(*S*)-Ibu-DAB-PSMA had a significant therapeutic advantage over [^{177}Lu]Lu-PSMA-617 and a favourable safety profile over [^{177}Lu]Lu-PSMA-ALB-56 [19]. The enantiopure [^{177}Lu]Lu-SibuDAB, modified with (*S*)-ibuprofen, demonstrated more favourable tumour-to-kidney ADC ratios and was, thus, selected for further development [20, 21].

The present study with [^{177}Lu]Lu-SibuDAB was aimed at determining the dosimetry in patients diagnosed with mCRPC and no other treatment option. Additionally, the safety profile was assessed by recording adverse events and monitoring blood parameters before and after treatment with [^{177}Lu]Lu-SibuDAB.

Material and methods

Study design and ethical approval

This prospective open-label single-arm investigator-initiated trial was designed to evaluate the biodistribution, dosimetry (primary objectives), preliminary safety and efficacy (secondary objectives) of [^{177}Lu]Lu-SibuDAB in patients with mCRPC, as well as changes in quality of life and pain scores (additional objectives). The study was approved by the regional ethics committee in Santiago de Chile, Chile. All patients gave written informed consent, and all reported investigations were conducted in accordance with the Declaration of Helsinki and local regulations.

Recruitment and inclusion criteria

Suitable candidates were recruited from the Hospital Clínico San Borja Arriarán of the University of Chile and referring hospitals within the greater area of Santiago de Chile. Patients with mCRPC were considered for participation in the study if (i) the disease was confirmed by PET/CT using [^{18}F]PSMA-1007, (ii) the levels of prostate-specific antigen (PSA) were rising according to Prostate Cancer Working Group 3 criteria [22–24] and (iii) no other available treatment options were available. Formal inclusion and exclusion criteria and the imaging protocol are listed in the Supplementary material.

Preparation of [^{177}Lu]Lu-SibuDAB

Good Manufacturing Practices-grade SibuDAB (Diverchim CDMO, Roissy-en-France, France) and non-carrier-added lutetium-177 (Isotope Technologies Munich SE, Garching, Germany) were used for the preparation of [^{177}Lu]Lu-SibuDAB. The radiolabelling was performed on an automated radiosynthesis module (Gaia V2 and Luna, Elysia-Raytest, Straubenhardt, Germany) with cassettes and reagent kits for ^{177}Lu-labeling (Advanced biochemical compounds ABX, Radeberg, Germany). Details on the radiosynthesis are given in the Supplementary material.

Treatment with [^{177}Lu]Lu-SibuDAB

Enrolled patients received up to 4 cycles of 5−6 GBq [^{177}Lu]Lu-SibuDAB as intravenous injection with an interval of 8−10 weeks between each cycle. Dosimetry was carried out during the first treatment cycle. To assess the association between

the administered mass of SibuDAB and the absorbed dose to normal organs and tumours, patients initially received a randomly assigned formulation of [^{177}Lu]Lu-SibuDAB containing one of three ligand mass levels (80 µg, 200 µg, 400 µg). Subsequent administrations contained 200 µg SibuDAB ligand mass.

Dosimetry

Whole-body (top of the skull to mid-thigh) SPECT/CT images were acquired on a Siemens Symbia SPECT/CT system (Siemens Healthineers, Erlangen, Germany) at nominal timepoints 1.5, 6, 24, 48, 168 h post-injection (p.i.) of [^{177}Lu]Lu-SibuDAB. The main acquisition parameters were: 45 stops (90 projections per energy window) over 360° (4° sampling) with 25 s dwell time per stop. Medium energy low penetration collimators were used, the main energy window was set as 187–229 keV, with upper and lower scatter windows. SPECT images were reconstructed iteratively with the system manufacturer's implementations (4.8 x 4.8 mm matrix, Flash 3D reconstruction, 8 iterations, 9 subsets, no post-reconstruction filtering) and corrected for scattered (triple energy windows) and attenuated photons (CT-based attenuation correction). Whole-body CT was acquired in a low-dose setting (80 mAs effective, 130 kVp, CareDose4D: on). Calibration factors were determined from a phantom acquisition under identical acquisition and reconstruction settings. Reconstructed SPECT and CT data were uploaded to a Hermia workstation (Hermes Medical Solutions, Stockholm, Sweden) for analysis.

Dosimetry was carried out based on sequential whole-body SPECT/CT imaging and venous blood sampling according to the principles outlined by the European Association of Nuclear Medicine dosimetry committee [25] using the implementation of OLINDA/EXM™ available in Hermes. Briefly, co-registration of SPECT and CT images was examined per timepoint for correctness and adapted if necessary. Sequential SPECT/CT datasets were loaded into the Hybrid Dosimetry application and co-registered. Analysed organs and tissues included the salivary glands (left and right parotid and submandibular glands), liver, spleen, kidneys (left and right), total body, and up to three tumour lesions per patient selected by the investigators. Volumes of interest around organs and tumour lesions were manually defined guided by CT and propagated to all SPECT images and were drawn to include also activity spilled out from the CT defined organ boundaries to compensate for the partial volume effect. Total activity in the patient was derived from the sum of all counts in the reconstructed SPECT. The mass of regions was independently determined on the CT images (24 h timepoint) for kidneys (medulla and cortex only), liver, spleen, and tumours. The total body mass was taken from the most up-to-date weight measurements for the respective patient. The individual mass of salivary glands was obtained by scaling the salivary gland mass of the adult male standard phantom (ICRP89 [26]) to the weight of each respective patient since direct volumetric measurement was impossible due to streak-artifacts in the low-dose CT images caused by dental implants. The mass of the red marrow was obtained in an equivalent fashion.

Venous blood samples ($n = 3$ for each timepoint) were drawn from the cubital vein at nominal timepoints 5, 15, 30 min, and 1.5, 6, 24, 48, 168 h p.i. The activity in the samples was measured using a calibrated γ-spectrometer (Elysia-Raytest, Mucha). The activity concentration (kBq/gram) was obtained by weighing the blood samples.

Time activity-curves (TACs) and time-integrated activity coefficients (TIACs)

Time-activity curves (TACs) and time-integrated activity coefficients (TIACs) for salivary glands, liver, spleen, kidneys, total body, and tumour lesions were directly obtained from the Hermes Hybrid Dosimetry application by fitting either bi-exponential or mono-exponential functions.

TACs for red marrow were obtained using the blood-specific activity and extrapolating to activity in the entire red marrow by multiplication with the red marrow mass. Thus, it was assumed that the activity concentration in red marrow is equal to the activity concentration in blood (red marrow to blood ratio = 1) [27]. Bi-exponential functions were fitted to non-decay corrected uptakes in GraphPad Prism (GraphPad Software LLC, version 10.1.2).

TIAC for organs, total body and tumour lesions were obtained by integration of TACs within either Hermes or GraphPad Prism.

Calculations of the absorbed dose

Obtained TIACs were used as input in the kinetics tab in OLINDA software (version 2.2.3, Hermes Medical Solutions, Stockholm, Sweden). The adult male standard phantom (ICRP89 [26]) was selected for the calculation of the absorbed dose and ADCs. The dose conversion factors in OLINDA were scaled by organ masses based on volumetric measurements as implemented in the software. The masses of all structures/organs that were not determined independently on imaging were scaled to the actual patient weight.

Additionally, the ADC for red marrow, assuming identical activity concentration in red marrow and blood and without any cross-irradiation from other sources was calculated separately. The latter has been termed *red marrow self*, while the absorbed dose including cross-irradiation from other sources was termed *red marrow total*. The spherical

model of OLINDA was applied for calculations of ADC to tumours.

Statistical analysis

Descriptive statistics are provided in the format (arithmetic mean) ± (standard deviation [SD]) or as median value and interquartile range where indicated. The association between variables was either assessed by a Kruskal-Wallis test for comparing the absorbed doses in the three different peptide mass groups or by Pearson correlation analysis for the dependence of absorbed dose on total tumour uptake. In general, two-sided p-values of less than a significance level of $\alpha = 0.05$ were considered statistically significant with Bonferroni adjustment for multiple testing. Association analyses were carried out in GraphPad Prism (GraphPad Software LLC, version 10.1.2).

Preliminary safety after first treatment cycle

Safety was evaluated by blood biomarker analysis and recording of adverse events by the principal investigator according to Common Terminology Criteria for Adverse Events v5.0 guidelines (published by National Institutes of Health, National Cancer Institute, Cancer Therapy Evaluation Program). Efficacy was assessed by pre- and post-therapeutic PET/CT imaging using [^{18}F]PSMA-1007 based on RECIP criteria [28], blood biomarker analysis and considering clinical parameters. In addition, a retrospective analysis of total tumour uptake on PET was performed, according to Unterrainer et al. [29], as also briefly described in Supplementary material. Herein, only the safety data covering the period after administration of the RPT until (excluding) the second treatment cycle will be reported. Further information on safety and efficacy will be shared in a follow-up publication.

Results

Patients and treatment regimen

Seventeen patients diagnosed with mCRPC (median serum PSA level 49.2 ng/mL, median standardised uptake value (standardised to body weight) ($SUV_{Mean-bw}$) of 7.4, median total tumour volume of 225.5 mL) were included in the study (Table 1). Up to 4 cycles of [^{177}Lu]Lu-SibuDAB were administered between June 2021 and January 2023 at the Center for Nuclear Medicine, Positronmed in Santiago de Chile, Chile. Data of sixteen patients were used for dosimetry assessment at the first treatment cycle while one patient was unable to undergo the necessary γ-camera acquisitions due to tumour

Table 1 Baseline information of patients treated with [^{177}Lu]Lu-SibuDAB

Patient characteristics[a]	
Median age (IQR) [years]	72 (63–83)
Median pre-treatment PSA value (IQR) [ng/mL]	49.2 (4.8–87.4)
Median total tumour uptake (IQR) [SUV*mL]	2,084.00 (590.50–10,957.75)
Disease sites	
Bone	16/17
Lymph nodes	11/17
Viscera	6/17
Prostate	11/17
Median injected activity (IQR) [GBq]	5.4 (5.1–5.6)
Median cycles of treatment (IQR)	3 (1–4)
Precursor mass[b]	
80 µg	5/17
200 µg	6/17
400 µg	6/17
Previous lines of therapy[c]	
0	1/16
1	2/16
2	7/16
3	2/16
4	4/16
Types of previous lines of therapy[c]	
Chemotherapy	
Docetaxel	12/16
Cabazitaxel	5/16
Docetaxel and Cabazitaxel	4/16
ARAT/ADT agents[c]	
Enzalutamide	4/16
Abiraterone	9/16
Bicalutamide	3/16
Other[d]	2/16
RPT ([^{177}Lu]Lu-PSMA-617, 4x)	1/16
Other previous treatments[c]	
Surgery	Yes: 5; No: 11
Radiotherapy (all)	Yes: 13; No: 3
Curative RT (alone)	*Yes: 1; No: 15*
Brachytherapy	*Yes: 2; No: 14*
Adjuvant RT	*Yes: 4; No: 12*
Palliative RT	*Yes: 8; No: 8*
Hormone blockade therapy[c]	Yes: 16; No: 0
First line ARAT	*Yes: 8; No: 8*

[a]Ethnic information was not recorded for patients. $n = 17$ unless specified

[b]$n = 17$, information of precursor mass was recorded at dosing, only 16 patients underwent dosimetry assessment

[c]Information on previous treatments for one patient was not available

[d]Apalutamide, enzalutamide – pembrolizumab

ARAT Androgen receptor axis-targeted, *ADT* Androgen deprivation therapy, *IQR* Interquartile range, *RPT* Radiopharmaceutical therapy, *SUV* Standardised uptake value (standardised to body weight), *SUV*mL* Standardised uptake value multiplied by tumour volume

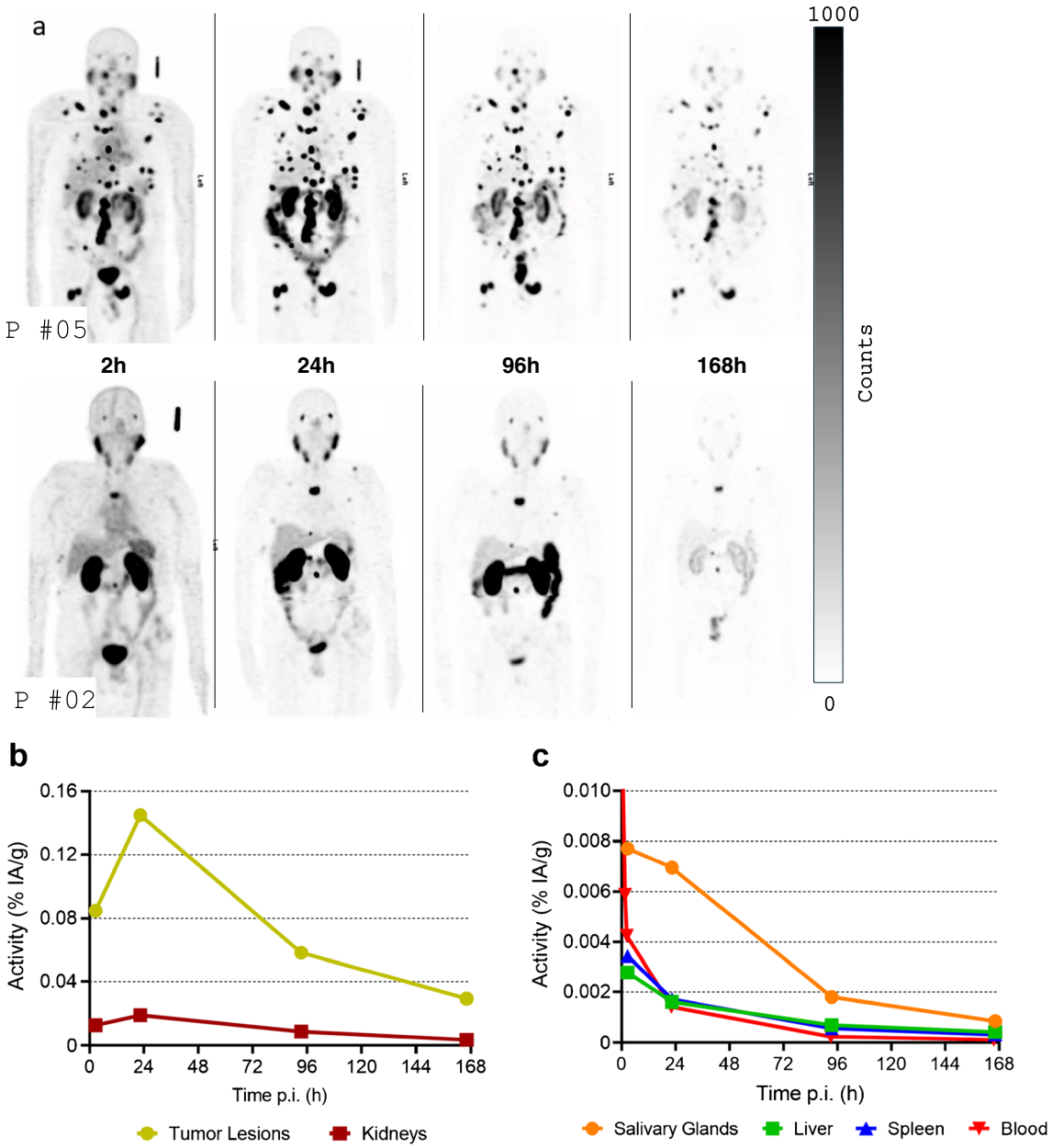

Fig. 1 **a** Maximum-intensity projections of SPECT images of [^{177}Lu]Lu-SibuDAB patient #5 (medium total tumour uptake) and patient #2 (low total tumour uptake), windowing at all timepoints was adjusted so that bottom (white) is 0 counts and top (black) is 1000 counts; **b** TACs for tumours and kidneys, expressed as percent injected activity per gram (% IA/g) for patient #5; **c** TACs for salivary glands, liver, spleen and red marrow (blood) (% IA/g) for patient #5. For better visualization, the initial peak of blood TAC is not shown. P = patient, p.i. = post injection; TAC = Time-activity curve

associated back pain. The administered activity for the treatment cycle with dosimetry was 5.3 ± 0.5 GBq of [^{177}Lu]Lu-SibuDAB.

Pharmacokinetics of [^{177}Lu]Lu-SibuDAB

On visual assessment, [^{177}Lu]Lu-SibuDAB exhibited a biodistribution pattern common to most small-molecule PSMA radiopharmaceuticals to date (Fig. 1a).

The highest uptake was observed in tumour lesions at ~ 24 h after injection of [^{177}Lu]Lu-SibuDAB, it was 9.2 ± 6.3 * 10^{-2}% IA/g, which was lower than the 13.4 ± 17.4 * 10^{-2}% IA/g reported for [^{177}Lu]Lu-PSMA-ALB-56 [17]. The uptake at ~ 24 h in the kidneys was 2.1 ± 0.6 * 10^{-2}% IA/g and in the salivary glands it was 0.6 ± 0.2 * 10^{-2}% IA/g, lower than for tumours and lower than for [^{177}Lu]Lu-PSMA-ALB-56 [17] (kidneys 2.3 ± 0.6 * 10^{-2}% IA/g, salivary glands 1.1 ± 0.5 * 10^{-2}% IA/g).

Table 2 Injected ligand mass and absorbed dose coefficients [Gy/GBq] for normal organs

Organ	Patient																Mean ± SD
Patient ID	1	2	3	4	5	6	7	8	9	10	11	12	13	14	15	16	
Ligand mass [µg]	200	200	200	200	200	200	400	400	400	400	80	80	80	80	80	400	
Kidneys	1.54	1.53	2.04	2.23	1.76	1.22	1.99	1.15	0.97	1.75	2.40	1.26	2.57	1.84	3.54	1.64	1.84 ± 0.64
Salivary glands	0.25	0.58	0.70	0.58	0.58	0.15	0.50	0.08	0.31	0.50	0.4	0.4	0.58	0.63	0.57	0.55	0.46 ± 0.18
Red marrow total	0.13	0.12	0.13	0.11	0.16	0.17	0.07	0.14	0.13	0.09	0.11	n.a.	0.07	0.06	0.08	0.04	0.10 ± 0.04
Red marrow self	0.1	0.06	0.07	0.07	0.07	0.05	0.04	0.03	0.02	0.04	0.07	n.a.	0.04	0.04	0.06	0.02	0.05 ± 0.02
Liver	n.a.	0.2	0.33	0.19	0.20	0.18	0.19	0.18	0.17	0.19	0.15	0.24	0.26	0.21	0.17	0.16	0.20 ± 0.05
Spleen	0.13	0.2	0.37	0.45	0.18	0.16	0.18	0.26	0.32	0.19	0.11	0.26	0.17	0.17	0.22	0.11	0.22 ± 0.09

n.a. not available

The activity concentration in the blood was 1.4 ± 0.4 * 10^{-2}% IA/g at 15 min post injection, 1.0 ± 0.3 * 10^{-2}% IA/g at 30 min, 0.3 ± 0.2 * 10^{-2}% IA/g at 6 h, 0.1 ± 0.1 * 10^{-2}% IA/g at 24 h and 0.009 ± 0.005 * 10^{-2}% IA/g at 7 days.

While the activity concentration in blood for the first time-point was only slightly lower than for ALB-56 [17] (1.6 ± 0.5 * 10^{-2}% IA/g at 15 min), it was considerably lower at later time-points (ALB-56: 0.5 ± 0.2 * 10^{-2}% IA/g at 6 h and 0.04 ± 0.01 * 10^{-2}% IA/g at 7 days), compatible with a faster clearance of [^{177}Lu]Lu-SibuDAB.

The TACs for tumour lesions, kidneys (both Fig. 1b) and blood, liver, spleen, salivary glands (all Fig. 1c) of one representative patient are provided.

Organ dosimetry

ADCs for [^{177}Lu]Lu-SibuDAB are given in Table 2. In non-tumour tissue, the highest ADC was observed for the kidneys with 1.84 ± 0.64 Gy/GBq (range 0.97−3.54 Gy/GBq), followed by salivary glands, spleen, liver, and red marrow total with 0.46 ± 0.18 Gy/GBq (range 0.08−0.7 Gy/GBq), 0.22 ± 0.09 Gy/GBq (range 0.11−0.45 Gy/GBq), 0.20 ± 0.05 Gy/GBq (range 0.15−0.33 Gy/GBq), and 0.10 ± 0.04 Gy/GBq (range 0.04−0.17 Gy/GBq), respectively. The ADC for red marrow self was 0.05 ± 0.02 Gy/GBq (range 0.02−0.12 Gy/GBq).

Tumour dosimetry

The ADC of 38 tumour lesions in 15 patients was determined (Table 3). In one patient (patient #13), tumour lesions could not be clearly distinguished from background in the SPECT/CT and were, thus, omitted for evaluation, the maximum-intensity-projections of PET and SPECT acquisitions of this patient are provided in Supplemental Fig. 1. The tumour doses showed a strong variation between individual lesions. The overall average ADC in tumour lesions was 9.9 ± 5.4 Gy/GBq (range: 0.8−27.6 Gy/GBq). The tumour-to-kidneys, tumour-to-salivary glands and tumour-to-red marrow ADC ratios were 6.7 ± 4.8, 33.1 ± 34.1, and 102 ± 81, respectively.

Association between injected ligand mass and absorbed dose coefficients

No significant differences between a particular SibuDAB ligand mass (Table 2) and the ADC for salivary glands, liver, spleen, kidneys, and tumours were found based on Kruskal-Wallis test and a multiple testing adjusted significance level of $\alpha = 0.0071$. The ADC for red marrow self was significantly different between the three ligand mass groups ($p = 0.0016$). An additionally performed Mann-Whitney test revealed that the 400 µg ligand mass group had a lower ADC for red marrow self (0.03 ± 0.01 Gy/GBq) as compared to the ADC for the 200 µg (0.07 ± 0.02 Gy/GBq) and 80 µg (0.05 ± 0.02 Gy/GBq) groups.

Association between total tumour uptake and absorbed dose coefficients

The total tumour uptake of [^{18}F]PSMA-1007 was determined in the pre-therapeutic PET/CT scans for each patient (Table 4 below; further details on PET/CT scan described in Supplementary material). Statistical significance ($p = 0.0004$) was found for the linear correlation (Pearson correlation analysis) of ADC to salivary glands and the total tumour uptake. Other tested associations between total tumour uptake and ADC to liver, spleen, kidneys, red marrow total, red marrow self, and tumours did not reach the multiple-testing adjusted significance level of $\alpha = 0.0071$. Scatter plots between total tumour uptake and ADC of several organs were prepared using the results of the Pearson correlation analysis (Fig. 2).

Table 3 Absorbed dose coefficients [Gy/GBq] and tumour-to-organ ADC ratios for all lesions

Tumour lesion	Patient																Mean ± SD[a]
	1	2	3	4	5	6	7	8	9	10	11	12	13	14	15	16	
1	6.2	6.0*	3.3*	8.3*	12.6*	10.6*	7.3*	12.4*	20.0*	4.8	14.0	9.4*	n.a.	3.4*	0.8*	11.5	
2	n.a.	4.6*	2.7*	12.4*	13.6*	10.0*	n.a.	8.2*	13.4*	6.4	16.2	16.6*	n.a.	19.0*	1.25	19.3	
3	n.a.	n.a.	n.a.	13.3*	8.9*	14.1*	n.a.	10.3*	22.4*	3.8*	27.6	21.5*	n.a.	3.18	n.a.	9.2	
Mean (all lesions)	6.2	5.3	3.0	11.3	11.7	11.6	7.3	10.3	18.6	5.0	19.3	15.8	n.a.	8.7	1.0	13.3	9.9 ± 5.4
Tumour/kidney ratio[b]	4.0	3.5	1.5	5.1	6.6	9.5	3.7	9.0	19.2	2.9	8.0	12.5	n.a.	4.7	0.3	8.1	6.6 ± 4.8
Tumour/salivary. glands[b, c]	24.8	9.1	4.3	19.5	20.2	77.3	14.6	128.8	60.0	10.0	48.3	39.5	n.a.	13.9	1.8	24.2	33.1 ± 34.1
Tumour/red marrow total[b]	47.7	44.2	23.1	102.7	73.1	68.2	104.3	73.6	143.1	55.6	175.5	n.a.	n.a.	145	12.5	332	102 ± 81

[a]Mean ± SD for tumour absorbed dose coefficients were calculated as mean across all individual lesions ($n = 38$ lesions in total)

[b]Tumour-to-organ ADC ratios were calculated as mean value of individual patient-based tumour-to-organ ratios, based on mean tumour absorbed dose coefficient for a patient

[c]Tumour-to-salivary gland ADC ratios were calculated based on mean absorbed dose across all four glands weighted equally

*bone lesions

ADC absorbed dose coefficient, *n.a.* not available

Table 4 Injected ligand mass of SibuDAB and total tumour uptake in pre-therapeutic [^{18}F]PSMA-1007 PET for all patients

Organ	Patient																Mean ± SD
Patient ID	1	2	3	4	5	6	7	8	9	10	16	11	12	13	14	15	
Ligand mass [µg]	200	200	200	200	200	200	400	400	400	400	400	80	80	80	80	80	
Total Tumour Uptake [SUV*mL]	718	98.7	1416	1000	4444	10902	65.1	21034	12598	2752	2882	11125	11640	841	280	89.1	5118 ± 6325
Group average Total Tumour Uptake [SUV*mL]	200 µg: 3096 ± 4113						400 µg: 7866 ± 8769					80 µg: 4795 ± 6022					

SUV Standardised uptake value (standardised to body weight), *SUV*mL* Standardised uptake value multiplied by tumour volume

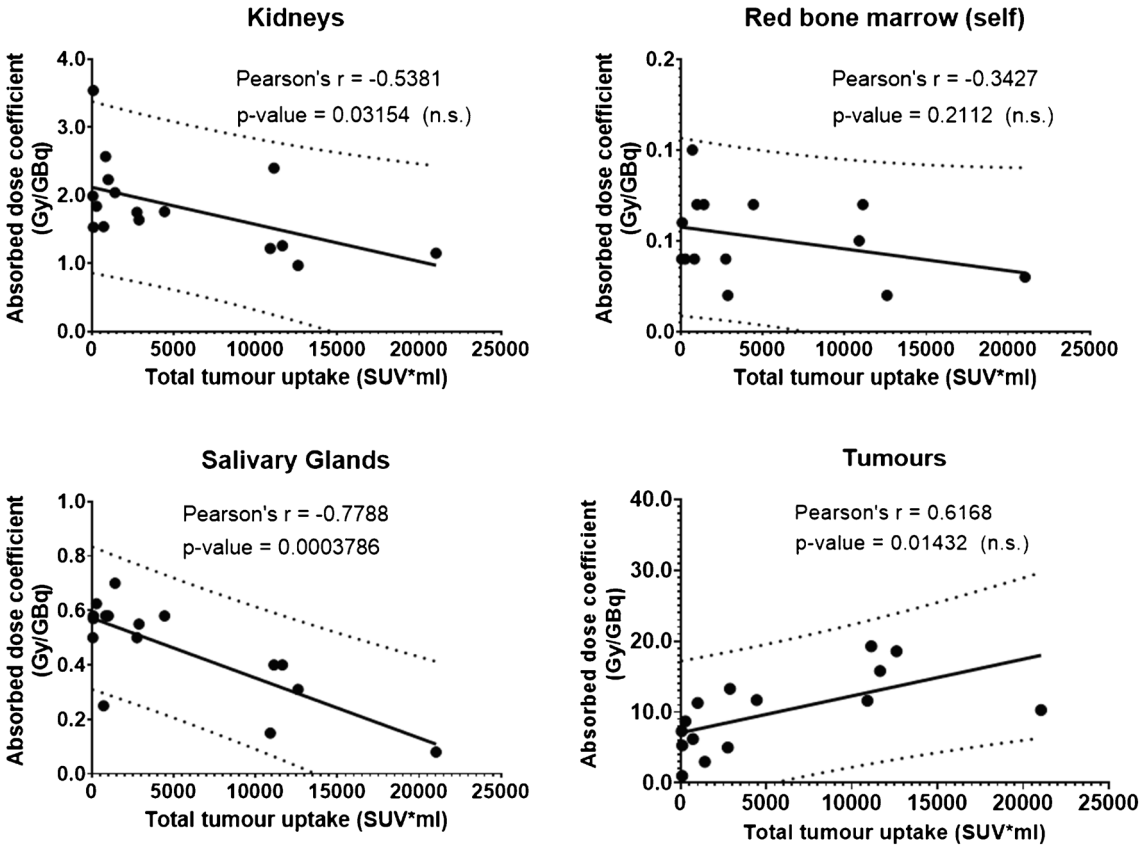

Fig. 2 Scatter plot for the association between total tumour uptake and absorbed dose coefficients for kidneys, red bone marrow (self), salivary glands, and tumours. The solid line represents the best line of fit and the dashed lines the 95% prediction interval. n.s. = not significant; SUV = Standardised uptake value (standardised to body weight); SUV*mL = Standardised uptake value multiplied by tumour volume

Safety of the first treatment cycle of [^{177}Lu]Lu-SibuDAB

The administration of [^{177}Lu]Lu-SibuDAB was safe and well tolerated by all patients. There were no adverse events or significant changes in vital signs on the day of the administration. During the follow-up until the second cycle of treatment (excluding), 7/17 patients (41%) developed or experienced an aggravation of an existing myelosuppression (including anaemia, thrombocytopenia, leukopenia, pancytopenia, among others). For two of these patients (12%) serious adverse events were recorded. One patient developed grade 3 anaemia and thrombocytopenia after an epistaxis event which was not related to the study drug. The second patient experienced grade 3 anaemia and grade 2 thrombocytopenia from grade 2 at baseline. Further non-severe adverse reactions included nausea (5/17), fatigue (5/17), and disease-related pain (5/17) due to extensive bone metastasis.

Discussion

Compared to other therapeutic PSMA radiopharmaceuticals, the ADC obtained for [^{177}Lu]Lu-SibuDAB were promising (Table 4), although a direct comparison was limited by the small sample sizes, heterogeneous instrumentation, and the inherent inaccuracies of dosimetry studies [30]. In line with the increased tumour uptake observed in preclinical studies, the tumour ADC was considerably higher for [^{177}Lu]Lu-SibuDAB (9.9 Gy/GBq) than for [^{177}Lu]Lu-PSMA-617 (3.6–4.2 Gy/GBq) [31] and [^{177}Lu]Lu-PSMA-I&T (2.9–4.1 Gy/GBq) [31]. Mean tumour-to-kidney ADC ratios of [^{177}Lu]Lu-SibuDAB (6.6) were in a similar range to those of [^{177}Lu]Lu-PSMA-617 (6.2–7.2) and [^{177}Lu]Lu-PSMA-I&T (4.1–5.8) (Table 5).

Importantly, a substantially improved tumour-to-salivary gland ADC ratio was obtained for [^{177}Lu]Lu-SibuDAB (33.1) when compared to other previously translated PSMA radiopharmaceuticals, such as [^{177}Lu]Lu-PSMA-617 (4.3–5.7) and [^{177}Lu]Lu-PSMA-I&T (4.6–9.5) (Table 5).

Table 5 Comparison of dosimetry data for different PSMA-targeting radiopharmaceuticals, currently under clinical investigation

	[^{177}Lu]Lu-SibuDAB	[^{177}Lu]Lu-PSMA-ALB-56	[^{177}Lu]Lu-EB-PSMA-617	[^{177}Lu]Lu-LNC1003	[^{177}Lu]Lu-PSMA-617	[^{177}Lu]Lu-PSMA-I&T	[^{177}Lu]Lu-J591
Reference	this report	Kramer et al. [17]	Zang et al. [32]	Zang et al. [33]	Ells et al. [31]	Ells et al. [31]	Vallabhajosula et al. [34]
ADC Kidneys (Gy/GBq)	1.84 (0.64)	2.54 (0.94)	2.38 (0.69)	2.24 (0.081)	0.58[b]	0.71[b]	1.41 (0.35)
ADC Red marrow (Gy/GBq)	0.10 (0.04)	0.29 (0.07)	0.054 (0.006)	0.22 (0.04)	0.03[b]	0.03[b]	0.32 (0.10)
ADC Salivary glands (Gy/GBq)	0.46 (0.18)	0.86 (0.42)	6.41 (1.40)	3.61 (2.83)	Parotid: 0.84[b] Submandib.: 0.74[b]	Parotid: 0.43[b] Submandib.: 0.64[b]	n.a.
ADC Tumour (Gy/GBq)	9.9 (5.4)	14.3 (25.2)	n.a.	Bone: 8.52 (4.20) Lymph node: 9.51 (2.02)	Bone: 3.57[b] Soft tissue: 4.19[b]	Bone: 4.10[b] Soft tissue: 2.94[b]	n.a.
Tumour-to-kidneys ADC ratio	6.6	5.6	n.a.	3.8–4.2[a]	6.2–7.2[a]	4.1–5.8[a]	n.a.
Tumour-to-red-marrow ADC ratio	102	49.3	n.a.	38.7–43.2[a]	119–139[a]	98–137[a]	n.a.
Tumour-to-salivary glands ADC ratio	33.1	16.6	n.a.	2.3–2.6[a]	4.3–5.7[a]	4.6–9.5[a]	n.a.

Absorbed doses are presented as mean (SD) values

[a]not directly available in reference, range calculated based on values in this table

[b]mean value reported, confidence intervals are available in reference

ADC absorbed dose coefficient, *n.a.* not available in the respective reference

Considering that xerostomia (grade 1 + 2) was observed as a frequent adverse event of [^{177}Lu]Lu-PSMA-617 therapy [35] and the severity is increasing for [^{225}Ac]Ac-radiolabelled PSMA-targeting, small-molecule inhibitors [36], this could be of clinical relevance in view of the clinical application of SibuDAB due to a high tumour-to-salivary gland ADC ratio. Consequently, SibuDAB labelled with terbium-161 (NCT06343038) and ^{225}Ac (ACTRN12624001123538) are currently being tested or planned to be tested in clinics.

Still, the exact mechanism for the higher tumour-to-salivary glands ratio is unclear. This could be due to higher tumour uptake for [^{177}Lu]Lu-SibuDAB over [^{177}Lu]Lu-PSMA-617 and [^{177}Lu]Lu-PSMA-I&T, a lower salivary gland uptake, an increased tumour sink effect due to the higher tumour uptake, or a combination of multiple factors. For example, one could hypothesize that the larger size of [^{177}Lu]Lu-SibuDAB as compared to [^{177}Lu]Lu-PSMA-617 and [^{177}Lu]Lu-PSMA-I&T reduces uptake in salivary glands, as for large PSMA-radioimmunoconjugates, no or only very low salivary gland uptake was reported [34].

As a result of the albumin-binding properties of [^{177}Lu]Lu-SibuDAB, the red bone marrow ADC dose was increased over that of [^{177}Lu]Lu-PSMA-617. Together with the increased tumour ADC for [^{177}Lu]Lu-SibuDAB this leading effectively to a slightly lower tumour-to-red marrow ADC ratio of 102 compared to 119–139 for [^{177}Lu]Lu-PSMA-617 (Table 5). In the present investigation, however, the red bone marrow-to-blood ratio was arbitrarily set to the most conservative assumption of 1.0, while other studies used lower factors such as 0.36 [34, 37–39] or even 0.32 [32]. The estimates of the present study may, thus, overestimate the dose received by the red bone marrow and the potential clinical impact. Still, [^{177}Lu]Lu-SibuDAB clearly has a slower clearance from blood than does [^{177}Lu]Lu-PSMA-617. At 24 h and 7 d post injection, the activity concentration in blood was 14% and 0.9% of its value at 30 min post injection for [^{177}Lu]Lu-SibuDAB, whereas it was reported to be 7% at 24 h and 0.4% at 6 d post injection for [^{177}Lu]Lu-PSMA-617 [40]. It should be noted that the topic of correct red bone marrow dosimetry for PSMA is discussed controversially, since many publications still rely on blood-based methods (e.g. Herrmann et al. [40]) and others apply image based techniques. To remain consistent with most literature and

Table 6 Comparison of biodistribution (TIAC) and dosimetry data (ADC) for different, albumin-binding PSMA-targeting radiopharmaceuticals and in different species

	Kidneys		Blood/Red Marrow		Tumours	
	Mouse TIAC [% IA/g*h]	Human ADC [Gy/GBq]	Mouse TIAC [% IA/g*h]	Human ADC [Gy/GBq]	Mouse TIAC [% IA/g*h]	Human ADC [Gy/GBq]
[^{177} Lu]Lu-PSMA-ALB-56	809	2.54	341	0.29	8491	14.3
[^{177} Lu]Lu-SibuDAB	433	1.84	78.55	0.1	6931	9.9
Change	−46%	−28%	−77%	−66%	−18%	−31%

ADC absorbed dose coefficient, *TIAC* time-integrated activity coefficients

previous work of the investigators [17], we opted for the blood-based approach.

In comparison to [^{177}Lu]Lu-PSMA-ALB-56 [15], [^{177}Lu]Lu-SibuDAB showed mostly improved pharmacokinetics, indicating that modulating the albumin-binding affinity to fine-tune the in vivo properties is a valid strategy for the development of radiopharmaceuticals. The mean absorbed dose to tumours and kidneys, respectively, was 31% and 28% lower after injection of [^{177}Lu]Lu-SibuDAB than after using [^{177}Lu]Lu-PSMA-ALB-56 [15, 17] resulting in similar tumour-to-kidney ADC ratios of 6.6 and 5.6 for the two radiopharmaceuticals (Table 5). The red bone marrow ADC was 66% lower for [^{177}Lu]Lu-SibuDAB than for [^{177}Lu]Lu-PSMA-ALB-56 resulting in a substantially improved tumour-to-red marrow ADC ratio of 102 for [^{177}Lu]Lu-SibuDAB versus 49.3 for [^{177}Lu]Lu-PSMA-ALB-56 (Table 5). These data are in line with the expectations based on preclinical data [15, 20, 21], demonstrated by good concordance of the preclinical TIACs of organs and clinical ADC (Table 6).

Previous attempts of translating PSMA-targeting radiopharmaceuticals with a longer blood plasma half-life to clinics refer to [^{177}Lu]Lu-EB-PSMA-617 [32] and [^{177}Lu]Lu-LNC1003 [33], both modified with Evans blue as an albumin-binding entity and the radioimmunoconjugate, [^{177}Lu]Lu-J591 [34]. A direct comparison of the data of the present study with those of [^{177}Lu]Lu-EB-PSMA-617 was not feasible due to the lack of tumour dosimetry data for the latter [32]. [^{177}Lu]Lu-SibuDAB, however, outperformed [^{177}Lu]Lu-LNC1003 based on available data of tumour-to-red marrow, tumour-to-kidney, and tumour-to-salivary gland ADC ratios. However, [^{177}Lu]Lu-J591 outperformed [^{177}Lu]Lu-SibuDAB regarding dosimetry data for the kidneys [34]. This can be ascribed to the fact that radioimmunoconjugates are not cleared through kidneys due to their large size [41]. On the other hand, [^{177}Lu]Lu-SibuDAB did not show the intense liver uptake that was seen after injection of [^{177}Lu]Lu-J591 in line with the hepatobiliary excretion of the latter. Importantly, the mean absorbed dose to the red marrow was about 3-fold lower for [^{177}Lu]Lu-SibuDAB (0.10 Gy/GBq) than for [^{177}Lu]Lu-J591 (0.32 Gy/GBq) [34], which is favourable, given the substantial myelosuppression observed in patients treated with [^{177}Lu]Lu-J591 [42].

In the present study, the choice of the injected activity was based on the previous experience with [^{177}Lu]Lu-PSMA-ALB-56 and [^{177}Lu]Lu-PSMA-617. Up to 24 GBq of [^{177}Lu]Lu-SibuDAB were administered and generally well tolerated. A detailed analysis of the safety data in this cohort will be published after collection of all data and adequate follow-up after last administration of [^{177}Lu]Lu-SibuDAB. Formal dose escalation studies will be necessary to determine the maximum tolerated activity for clinical routine, possibly aided by individual dosimetry [43].

Besides red marrow self doses, statistical analysis did not reveal significant differences in ADC between the three groups treated with different precursor masses. Hypothetically, an increased precursor mass could lead to saturation of PSMA-binding sites as it was demonstrated in preclinical studies [44]. The differences in red marrow dose between different ligand mass observed in the present study were, however, small and inconsistent in direction as the highest radiation doses were found in the intermediate ligand mass group.

The hypothesis that a varying extent of the tumour sink effect was a confounding factor, potentially interfering with consistency of data for specific precursor mass groups, was evaluated by determining tumour uptake in the pre-therapeutic [^{18}F]PSMA-1007 for PET/CT data since a large variation in total tumour uptake was detectable in the different precursor mass groups (Table 2). An extensive tumour burden and related uptake of the PSMA radiopharmaceutical may result in decreased off-target accumulation, an effect also known as “sink effect” [45, 46]. As observed in Fig. 2, there is a visual trend of decreasing ADC for kidneys, red marrow, and salivary glands for increasing total tumour uptake in the patient, compatible with a tumour sink effect. Only the linear regression between salivary gland ADC and total tumour uptake reached the required, multiple testing adjusted,

statistical significance level. For PSMA-avid tumours, one expects a positive correlation between uptake of [^{18}F]PSMA-1007 in the lesions and lesion absorbed dose of the ^{177}Lu-based PSMA radiopharmaceutical, as already previously reported [47]. This trend is as well visually evident (Fig. 2), but the linear correlation analysis did not reach the required statistical significance level. Still, due to the visually apparent trends for all analysed regions, it cannot be ruled out that the imbalance of total tumour uptake between the three different ligand mass groups potentially confounded the detection of a clear influence of ligand mass on absorbed doses. Clearly, larger cohorts of patients would be necessary to finally conclude on the most favourable ligand mass to be used for follow-up clinical studies.

Conclusion

This study demonstrated the generally favourable biodistribution profile of [^{177}Lu]LuSibuDAB in mCRPC patients with increased absorbed tumour doses while tumour-to-organ ADC ratios for kidneys and red bone marrow were in a similar range as for conventionally employed PSMA radiopharmaceuticals. Most relevant was the improved tumour-to-salivary gland ADC ratio as compared to that of [^{177}Lu]Lu-PSMA-617. [^{177}Lu]Lu-SibuDAB is a promising novel radiopharmaceutical with potential for further development in clinical trials.

Supplementary Information The online version contains supplementary material available at https://doi.org/10.1007/s00259-025-07102-8.

Acknowledgements The authors would like to thank all patients and their families for participation and contribution to the research presented here. They would like to thank Brahmasivasenkar Lingam and Wiebke Griemberg for medical writing support, Frano Poljak for supporting with the dosimetry evaluations, Johanna Wettlin for accompanying and supporting the patients during the study and Matias Ceballos for performing the SPECT/CT imaging studies. The authors thank Luisa M. Deberle, Francesca Borgna, Viviane J. Tschan and Sarah D. Busslinger as well as Susan Cohrs and Fan Sozzi-Guo for contributing to the preclinical studies and related reports to enable the translation of [^{177}Lu]Lu-SibuDAB to this clinical study.

Author Contributions Study conception and design: René Fernández, Cristian Soza-Ried, Heinz Nicolai, Horacio Amaral, Roger Schibli, Cristina Müller, Konstantin Zhernosekov, and Vasko Kramer.

Data collection: René Fernández, Cristian Soza-Ried, Heinz Nicolai, and Vasko Kramer.

Data evaluation: Philipp Ritt, René Fernández, Cristian Soza-Ried, Heinz Nicolai, Horacio Amaral, Korbinian Krieger, Ana Katrina Mapanao, Amanda Rotger, Cristina Müller, Vasko Kramer.

Drafting and revising the manuscript: All authors.

Approval of the final manuscript: All authors.

Funding Korbinian Krieger was supported by an ETH MedLab Fellowship and a research grant from the International Centers for Precision Oncology Foundation (ICPO, Germany). Ana Katrina Mapanao was funded by a SNSF grant (N° 310030_188978; PI: Cristina Müller) and by the European Union's Horizon 2020 research and innovation program under the Marie Skłodowska-Curie grant agreement N° 884104.

Data availability The datasets generated during and analysed during this study are covered by data protection regulation and cannot be distributed.

Declarations

Ethical approval All procedures performed in this study involving human patients were in accordance with the ethical standards of the institutional and national research committee and with the principles of the 1964 Declaration of Helsinki and its later amendments or comparable ethical standards. The study was approved by the regional ethics committee board (CEC SSM Oriente, permit 20210521) and written informed consent has been obtained from all individual patients included in the study.

Competing interests The authors declare the following competing financial interest(s): Patent applications on PSMA ligands with albumin-binding entities have been filed by ITM Medical Isotopes GmbH, Germany and the Paul Scherrer Institute, Switzerland. KZ, RS and CM are listed as co-inventors. The authors further declare non-financial interest(s): non-carrier-added lutetium-177 was provided by ITM Medical Isotopes GmbH, Germany.

References

1. Siegel RL, Miller KD, Fuchs HE, Jemal A. Cancer statistics, 2022. CA Cancer J Clin. 2022;72:7–33. https://doi.org/10.3322/caac.21708.
2. Ross JS, Sheehan CE, Fisher HA, Kaufman RP Jr., Kaur P, Gray K, et al. Correlation of primary tumor prostate-specific membrane antigen expression with disease recurrence in prostate cancer. Clin Cancer Res. 2003;9:6357–62.
3. Novakova Z, Foss CA, Copeland BT, Morath V, Baranova P, Havlinova B, et al. Novel monoclonal antibodies recognizing human prostate-specific membrane antigen (PSMA) as research and theranostic tools. Prostate. 2017;77:749–64. https://doi.org/10.1002/pros.23311.
4. Labriola MK, Atiq S, Hirshman N, Bitting RL. Management of men with metastatic castration-resistant prostate cancer following potent androgen receptor inhibition: a review of novel investigational therapies. Prostate Cancer Prostatic Dis. 2021;24:301–9. https://doi.org/10.1038/s41391-020-00299-9.
5. Haberkorn U, Eder M, Kopka K, Babich JW, Eisenhut M. New strategies in prostate cancer: prostate-specific membrane antigen

(PSMA) ligands for diagnosis and therapy. Clin Cancer Res. 2016;22:9–15. https://doi.org/10.1158/1078-0432.CCR-15-0820.
6. Eiber M, Fendler WP, Rowe SP, Calais J, Hofman MS, Maurer T, et al. Prostate-specific membrane antigen ligands for imaging and therapy. J Nucl Med. 2017;58:S67–76. https://doi.org/10.2967/jnumed.116.186767.
7. Kulkarni HR, Singh A, Schuchardt C, Niepsch K, Sayeg M, Leshch Y, et al. PSMA-based radioligand therapy for metastatic castration-resistant prostate cancer: the Bad Berka experience since 2013. J Nucl Med. 2016;57:S97–104. https://doi.org/10.2967/jnumed.115.170167.
8. Rahbar K, Ahmadzadehfar H, Kratochwil C, Haberkorn U, Schafers M, Essler M, et al. German multicenter study investigating ^{177}Lu-PSMA-617 radioligand therapy in advanced prostate cancer patients. J Nucl Med. 2017;58:85–90. https://doi.org/10.2967/jnumed.116.183194.
9. von Eyben FE, Roviello G, Kiljunen T, Uprimny C, Virgolini I, Kairemo K, et al. Third-line treatment and ^{177}Lu-PSMA radioligand therapy of metastatic castration-resistant prostate cancer: a systematic review. Eur J Nucl Med Mol Imaging. 2018;45:496–508. https://doi.org/10.1007/s00259-017-3895-x.
10. Heck MM, Tauber R, Schwaiger S, Retz M, D'Alessandria C, Maurer T, et al. Treatment outcome, toxicity, and predictive factors for radioligand therapy with ^{177}Lu-PSMA-I&T in metastatic castration-resistant prostate cancer. Eur Urol. 2019;75:920–6. https://doi.org/10.1016/j.eururo.2018.11.016.
11. Rasul S, Hartenbach M, Wollenweber T, Kretschmer-Chott E, Grubmuller B, Kramer G, et al. Prediction of response and survival after standardized treatment with 7400 MBq ^{177}Lu-PSMA-617 every 4 weeks in patients with metastatic castration-resistant prostate cancer. Eur J Nucl Med Mol Imaging. 2021;48:1650–7. https://doi.org/10.1007/s00259-020-05082-5.
12. Hennrich U, Eder M. [^{177}Lu]Lu-PSMA-617 (Pluvicto(TM)): The first FDA-approved radiotherapeutical for treatment of prostate cancer. Pharmaceuticals (Basel). 2022;15. https://doi.org/10.3390/ph15101292.
13. Dumelin CE, Trüssel S, Buller F, Trachsel E, Bootz F, Zhang Y, et al. A portable albumin binder from a DNA-encoded chemical library. Angew Chem Int Ed Engl. 2008;47:3196–201. https://doi.org/10.1002/anie.200704936.
14. Benesova M, Guzik P, Deberle LM, Busslinger SD, Landolt T, Schibli R, et al. Design and evaluation of novel albumin-binding folate radioconjugates: systematic approach of varying the linker entities. Mol Pharm. 2022;19:963–73. https://doi.org/10.1021/acs.molpharmaceut.1c00932.
15. Umbricht CA, Benesova M, Schibli R, Müller C. Preclinical development of novel PSMA-targeting radioligands: modulation of albumin-binding properties to improve prostate cancer therapy. Mol Pharm. 2018;15:2297–306. https://doi.org/10.1021/acs.molpharmaceut.8b00152.
16. Kelly J, Amor-Coarasa A, Ponnala S, Nikolopoulou A, Williams C Jr., Schlyer D, et al. Trifunctional PSMA-targeting constructs for prostate cancer with unprecedented localization to LNCaP tumors. Eur J Nucl Med Mol Imaging. 2018. https://doi.org/10.1007/s00259-018-4004-5.
17. Kramer V, Fernandez R, Lehnert W, Jimenez-Franco LD, Soza-Ried C, Eppard E, et al. Biodistribution and dosimetry of a single dose of albumin-binding ligand [^{177}Lu]Lu-PSMA-ALB-56 in patients with mCRPC. Eur J Nucl Med Mol Imaging. 2021;48:893–903. https://doi.org/10.1007/s00259-020-05022-3.
18. Deberle LM, Benesova M, Umbricht CA, Borgna F, Büchler M, Zhernosekov K, et al. Development of a new class of PSMA radioligands comprising ibuprofen as an albumin-binding entity. Theranostics. 2020;10:1678–93. https://doi.org/10.7150/thno.40482.
19. Tschan VJ, Borgna F, Busslinger SD, Stirn M, Rodriguez JMM, Bernhardt P, et al. Preclinical investigations using [^{177}Lu]Lu-IbuDAB-PSMA toward its clinical translation for radioligand therapy of prostate cancer. Eur J Nucl Med Mol Imaging. 2022;49:3639–50. https://doi.org/10.1007/s00259-022-05837-2.
20. Borgna F, Deberle LM, Busslinger SD, Tschan VJ, Walde LM, Becker AE, et al. Preclinical investigations to explore the difference between the diastereomers [^{177}Lu]Lu-SibuDAB and [^{177}Lu]Lu-RibuDAB toward prostate cancer therapy. Mol Pharm. 2022;19:2105–14. https://doi.org/10.1021/acs.molpharmaceut.1c00994.
21. Tschan VJ, Busslinger SD, Bernhardt P, Grundler PV, Zeevaart JR, Köster U, et al. Albumin-binding and conventional PSMA ligands in combination with ^{161}Tb: biodistribution, dosimetry, and preclinical therapy. J Nucl Med. 2023;64:1625–31. https://doi.org/10.2967/jnumed.123.265524.
22. Oken MM, Creech RH, Tormey DC, Horton J, Davis TE, McFadden ET, et al. Toxicity and response criteria of the Eastern Cooperative Oncology Group. Am J Clin Oncol. 1982;5:649–55.
23. Scher HI, Morris MJ, Stadler WM, Higano C, Basch E, Fizazi K, et al. Trial design and objectives for castration-resistant prostate cancer: updated recommendations from the prostate cancer clinical trials working group 3. J Clin Oncol. 2016;34:1402–18. https://doi.org/10.1200/JCO.2015.64.2702.
24. Giesel FL, Knorr K, Spohn F, Will L, Maurer T, Flechsig P, et al. Detection efficacy of ^{18}F-PSMA-1007 PET/CT in 251 patients with biochemical recurrence of prostate cancer after radical prostatectomy. J Nucl Med. 2019;60:362–8. https://doi.org/10.2967/jnumed.118.212233.
25. Sjögreen Gleisner K, Chouin N, Gabina PM, Cicone F, Gnesin S, Stokke C, et al. EANM dosimetry committee recommendations for dosimetry of ^{177}Lu-labelled somatostatin-receptor- and PSMA-targeting ligands. Eur J Nucl Med Mol Imaging. 2022;49:1778–809. https://doi.org/10.1007/s00259-022-05727-7.
26. Stabin MG, Xu XG, Emmons MA, Segars WP, Shi C, Fernald MJ. RADAR reference adult, pediatric, and pregnant female phantom series for internal and external dosimetry. J Nucl Med. 2012;53:1807–13. https://doi.org/10.2967/jnumed.112.106138.
27. Hindorf C, Glatting G, Chiesa C, Linden O, Flux G, Committee ED. EANM Dosimetry Committee guidelines for bone marrow and whole-body dosimetry. Eur J Nucl Med Mol Imaging. 2010;37:1238–50. https://doi.org/10.1007/s00259-010-1422-4.
28. Gafita A, Rauscher I, Weber M, Hadaschik B, Wang H, Armstrong WR, et al. Novel framework for treatment response evaluation using PSMA PET/CT in patients with metastatic castration-resistant prostate cancer (RECIP 1.0): an international multicenter study. J Nucl Med. 2022;63:1651–8. https://doi.org/10.2967/jnumed.121.263072.
29. Unterrainer LM, Beyer L, Zacherl MJ, Gildehaus FJ, Todica A, Kunte SC, et al. Total tumor volume on ^{18}F-PSMA-1007 PET as additional imaging biomarker in mCRPC patients undergoing PSMA-targeted alpha therapy with ^{225}Ac-PSMA-I&T. Biomedicines. 2022;10. https://doi.org/10.3390/biomedicines10050946.
30. Flux GD, Guy MJ, Beddows R, Pryor M, Flower MA. Estimation and implications of random errors in whole-body dosimetry for targeted radionuclide therapy. Phys Med Biol. 2002;47:3211–23. https://doi.org/10.1088/0031-9155/47/17/311.
31. Ells Z, Grogan TR, Czernin J, Dahlbom M, Calais J. Dosimetry of [^{177}Lu]Lu-PSMA-targeted radiopharmaceutical therapies in patients with prostate cancer: A comparative systematic review and metaanalysis. J Nucl Med. 2024. https://doi.org/10.2967/jnumed.124.267452.
32. Zang J, Fan X, Wang H, Liu Q, Wang J, Li H, et al. First-in-human study of ^{177}Lu-EB-PSMA-617 in patients with metastatic castration-resistant prostate cancer. Eur J Nucl Med Mol Imaging. 2019;46:148–58. https://doi.org/10.1007/s00259-018-4096-y.

33. Zang J, Wang G, Zhao T, Liu H, Lin X, Yang Y, et al. A phase 1 trial to determine the maximum tolerated dose and patient-specific dosimetry of [^{177}Lu]Lu-LNC1003 in patients with metastatic castration-resistant prostate cancer. Eur J Nucl Med Mol Imaging. 2024;51:871–82. https://doi.org/10.1007/s00259-023-06470-3.
34. Vallabhajosula S, Kuji I, Hamacher KA, Konishi S, Kostakoglu L, Kothari PA, et al. Pharmacokinetics and biodistribution of ^{111}In- and ^{177}Lu-labeled J591 antibody specific for prostate-specific membrane antigen: prediction of ^{90}Y-J591 radiation dosimetry based on ^{111}In or ^{177}Lu? J Nucl Med. 2005;46:634–41.
35. Chi KN, Armstrong AJ, Krause BJ, Herrmann K, Rahbar K, de Bono JS, et al. Safety analyses of the phase 3 VISION trial of [^{177}Lu]Lu-PSMA-617 in patients with metastatic castration-resistant prostate cancer. Eur Urol. 2024;85:382–91. https://doi.org/10.1016/j.eururo.2023.12.004.
36. Satapathy S, Sood A, Das CK, Mittal BR. Evolving role of ^{225}Ac-PSMA radioligand therapy in metastatic castration-resistant prostate cancer-a systematic review and meta-analysis. Prostate Cancer Prostatic Dis. 2021;24:880–90. https://doi.org/10.1038/s41391-021-00349-w.
37. Kratochwil C, Giesel FL, Stefanova M, Benesova M, Bronzel M, Afshar-Oromieh A, et al. PSMA-targeted radionuclide therapy of metastatic castration-resistant prostate cancer with ^{177}Lu-labeled PSMA-617. J Nucl Med. 2016;57:1170–6. https://doi.org/10.2967/jnumed.115.171397.
38. Delker A, Schleske M, Liubchenko G, Berg I, Zacherl MJ, Brendel M, et al. Biodistribution and dosimetry for combined [^{177}Lu]Lu-PSMA-I&T/[225Ac]Ac-PSMA-I&T therapy using multi-isotope quantitative SPECT imaging. Eur J Nucl Med Mol Imaging. 2023;50:1280–90. https://doi.org/10.1007/s00259-022-06092-1.
39. Kabasakal L, AbuQbeitah M, Aygun A, Yeyin N, Ocak M, Demirci E, et al. Pre-therapeutic dosimetry of normal organs and tissues of ^{177}Lu-PSMA-617 prostate-specific membrane antigen (PSMA) inhibitor in patients with castration-resistant prostate cancer. Eur J Nucl Med Mol Imaging. 2015;42:1976–83. https://doi.org/10.1007/s00259-015-3125-3.
40. Herrmann K, Rahbar K, Eiber M, Sparks R, Baca N, Krause BJ, et al. Renal and Multiorgan safety of ^{177}Lu-PSMA-617 in patients with metastatic castration-resistant prostate cancer in the VISION dosimetry substudy. J Nucl Med. 2024;65:71–8. https://doi.org/10.2967/jnumed.123.265448.
41. Chang SS, Reuter VE, Heston WD, Bander NH, Grauer LS, Gaudin PB. Five different anti-prostate-specific membrane antigen (PSMA) antibodies confirm PSMA expression in tumor-associated neovasculature. Cancer Res. 1999;59:3192–8.
42. Bander NH, Milowsky MI, Nanus DM, Kostakoglu L, Vallabhajosula S, Goldsmith SJ. Phase I trial of ^{177}lutetium-labeled J591, a monoclonal antibody to prostate-specific membrane antigen, in patients with androgen-independent prostate cancer. J Clin Oncol. 2005;23:4591–601. https://doi.org/10.1200/JCO.2005.05.160.
43. Brosch-Lenz J, Delker A, Volter F, Unterrainer LM, Kaiser L, Bartenstein P, et al. Toward single-time-point image-based dosimetry of ^{177}Lu-PSMA-617 therapy. J Nucl Med. 2023;64:767–74. https://doi.org/10.2967/jnumed.122.264594.
44. Tschan VJ, Borgna F, Schibli R, Müller C. Impact of the mouse model and molar amount of injected ligand on the tissue distribution profile of PSMA radioligands. Eur J Nucl Med Mol Imaging. 2022;49:470–80. https://doi.org/10.1007/s00259-021-05446-5.
45. Schmidkonz C, Cordes M, Schmidt D, Bauerle T, Goetz TI, Beck M, et al. ^{68}Ga-PSMA-11 PET/CT-derived metabolic parameters for determination of whole-body tumor burden and treatment response in prostate cancer. Eur J Nucl Med Mol Imaging. 2018;45:1862–72. https://doi.org/10.1007/s00259-018-4042-z.
46. Gafita A, Wang H, Robertson A, Armstrong WR, Zaum R, Weber M, et al. Tumor sink effect in ^{68}Ga-PSMA-11 PET: myth or reality? J Nucl Med. 2022;63:226–32. https://doi.org/10.2967/jnumed.121.261906.
47. Violet J, Jackson P, Ferdinandus J, Sandhu S, Akhurst T, Iravani A, et al. Dosimetry of ^{177}Lu-PSMA-617 in metastatic castration-resistant prostate cancer: correlations between pretherapeutic imaging and whole-body tumor dosimetry with treatment outcomes. J Nucl Med. 2019;60:517–23. https://doi.org/10.2967/jnumed.118.219352.

Authors and Affiliations

Philipp Ritt[1,2] · René Fernández[3] · Cristian Soza-Ried[3,4] · Heinz Nicolai[3,5] · Horacio Amaral[3,6] · Korbinian Krieger[7,8] · Ana Katrina Mapanao[7] · Amanda Rotger[1] · Konstantin Zhernosekov[1] · Roger Schibli[7,8] · Cristina Müller[7,8] · Vasko Kramer[3,6]

✉ Philipp Ritt
philipp.ritt@itm-radiopharma.com

[1] ITM Oncologics GmbH, Lichtenbergstrasse 1, 85748 Garching, Munich, Germany

[2] Chair for Clinical Nuclear Medicine, Friedrich-Alexander-Universität Erlangen-Nürnberg, 91054 Erlangen, Germany

[3] Center for Nuclear Medicine & PET/CT Positronmed, 7501068 Providencia, Santiago, Chile

[4] Facultad de Medicina Veterinaria y Agronomía, Instituto de Ciencias Naturales, Universidad de las Américas, Santiago, Chile

[5] Departamento de Urología, Hospital Clínico San Borja Arriarán, Universidad de Chile, Santiago, Chile

[6] Positronpharma SA, 7501068 Providencia, Santiago, Chile

[7] Center for Radiopharmaceutical Sciences, PSI Center for Life Sciences, 5232 Villigen-PSI, Switzerland

[8] Department of Chemistry and Applied Biosciences, ETH Zurich, 8093 Zurich, Switzerland